

Shell-type Supernova Remnants

Heinrich J. Völk

Max-Planck-Institut für Kernphysik
P.O. Box 103980
D-69029 Heidelberg, Germany

The role of Supernova Remnants (SNRs) for the production of the Galactic Cosmic Rays is reviewed from the point of view of theory and very high energy gamma-ray experiments. The point is made that theory can describe young SNRs very well, if the evidence from the synchrotron emission is used to empirically determine several parameters of the theory, and thus theory can predict the relative contributions of hadronic and leptonic gamma rays at TeV energies. This is exemplified for several objects that have been observed intensively during the last years. Future key observations are discussed.

1 Introduction

Shell-type supernova remnants (SNRs) are widely assumed to be the sources of the Cosmic Rays (CRs), as they are observed in the neighborhood of the Solar System. This concerns particle energies up to the "knee" of the energy spectrum at several 10^{15} eV or possibly beyond (see [1] for a recent review). From estimates of the Galactic Supernova (SN) rate and the CR escape rate from the Galaxy SNRs have then to convert on average about 10% of their entire mechanical explosion energy into CRs – an enormous requirement.

A direct experimental investigation of SNRs as CR sources is possible with γ -ray observations at very high energies > 100 GeV (VHE). The argument is the following: the acceleration of particles to CR energies is assumed to occur primarily at the outer,

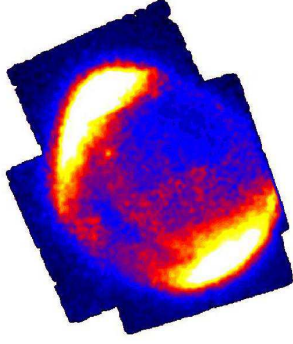


Figure 1: *ASCA* image of SN 1006 in hard X-rays from [2]. The emission comes mainly from the North-eastern and Southwestern areas, interpreted as polar caps, where the mean magnetic field is quasi-parallel to the shock normal of the outer SNR blast wave [3]. The resolution of *ASCA* is slightly better than that of the *H.E.S.S.* array, indicating what is presently achievable in VHE γ -rays.

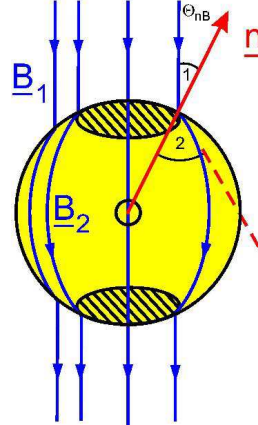


Figure 2: Schematic of the average magnetic field geometry for a SN explosion into a uniform interstellar medium with a homogenous field \underline{B}_1 . Θ_{nB} is the angle between the shock normal vector \underline{n} and \underline{B}_1 . Injection of downstream suprathermal ion is only possible for sufficiently small values of Θ_{nB} , i.e. in the hatched polar regions.

quasi-spherical shock which also compresses and heats the ambient circumstellar medium. The expanding shock wave confines the accelerated particles in its interior until its velocity decreases substantially at late times. Then the shock gets “old” and the more energetic particles successively leave the remnant. There fore a distant γ -ray observer of a “young” SNRs can see the π^0 -decay and nonthermal Bremsstrahlung (NB) emission, due to CR collisions with gas particles in the interior, jointly with the Inverse Compton (IC) radiation as originating from a *localized* source. Together with the electron synchrotron spectrum – from radio to hard X-ray energies – and the synchrotron morphology (e.g. Fig. 1) this is

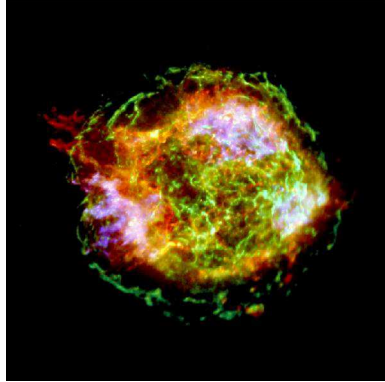


Figure 3: *Cas A in X-ray synchrotron light, observed with Chandra.* Image courtesy of NASA/CXG/GSFC/U.Hwang et al..

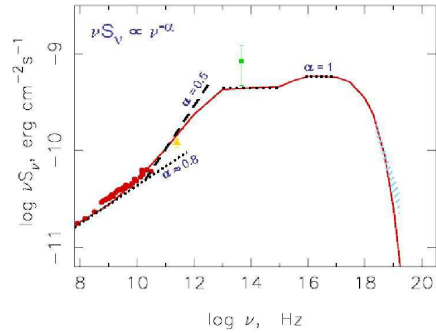


Figure 4: *Synchrotron spectral energy density (SED) of Cas A: data and theoretical spectrum [15].* The low-frequency photon spectrum has a spectral index $\alpha \approx 0.8$ (dotted curve), not quite increasing to the test particle value $\alpha \approx 0.5$ before in the sub-mm region the electrons inside the SNR are already radiatively cooled, so that $\alpha \approx 1$ before the cutoff.

the nonthermal electromagnetic evidence. I want to argue below that the synchrotron emission allows us to separate the contributions of nuclear CRs and ultrarelativistic CR electrons to the γ -ray emission; in addition, we can then determine key theoretical quantities like the effective magnetic field and the rate of injection of suprathermal ions into the acceleration process. In this way it becomes possible to calculate the energy density and the energy spectrum of nuclear CRs in the SNR from theory. To obtain quantitative results, obviously some further astronomical multi-wave-length (MWL) information is required. This concerns the source distance, the angular size/morphology, the SNR expansion rate, and the circumstellar density structure. SNe also result from two basically different physical processes whose main manifestations are type Ia

explosions (deflagration/detonation of an accreting White Dwarf) and type II explosions (core collapse of a massive star), with several variants according to the mass of the progenitor star. These different SN types are connected with different magnitudes of the ejected mass. Therefore also the explosion type must be known from astronomical measurements.

In this talk I will review the general status of the γ -ray observations, emphasizing the non-spherical aspects of the nonthermal emission from SNRs and the relation of theory and experiment in this field. In this light I will describe four major sources: Cas A, SN 1006, RX J1713.7-3946, and Vela Jr. I will end with a short discussion of the contribution to nonthermal SNR research by the recent Galactic Plane Scan, performed with the *H.E.S.S.* experiment. In some respects this is an extension of a paper given at the 28th ICRC in Tsukuba [4].

2 Gamma-ray detectability of SNRs and their non-spherical aspects

The *EGRET* instrument on the *Compton Gamma Ray Observatory (CGRO)* has not been able to find unequivocal evidence for γ -ray emission from SNRs in its energy range below a few GeV. The reasons are the low source flux, even for objects as close as 1 kpc, and the large angular extent of $\sim 1^\circ$ – of the order of the diameter of the full Moon – which implies a high γ -ray background from diffuse Galactic CRs. If we anticipate the particle energy spectra in the sources to be much harder than the energy spectra of the diffuse Galactic CRs, then the signal-to-background ratio decreases with decreasing γ -ray energy, making the GeV range generally unfavorable for detection. In contrast, ground-based imaging Cherenkov telescopes have made several detections in dedicated VHE observations (see section 4), and the *H.E.S.S.* experiment

has identified SNR counterparts for several sources found in its Galactic Plane Survey. The reasons are the large effective area of these telescopes/telescope systems, the relatively lower diffuse γ -ray background at TeV energies, and the much better angular resolution of $\sim 10^{-1}$ degrees compared to *EGRET*. This makes nearby SNRs at least marginally detectable [5].

2.1 Non-spherical aspects of SNRs

Theoretical models for diffusive shock acceleration at SNRs face the difficulty of having to cope with the fundamentally non-planar and even non-spherical geometry of a point explosion into an environment that lacks spherical symmetry. The dynamics is described by kinetic equations for the particle distributions $f(p, r, t)$ as functions of particle momentum p , radial distance r and time t , nonlinearly coupled with the hydrodynamics of the thermal gas. Only spherically symmetric solutions are available until now which solve this intrinsically time-dependent problem [6, 7]. It is clear on the other hand that the magnetic field, which regulates the particle injection rate into the acceleration process, cannot be spherically symmetric and is even on average at best axially symmetric in SNRs.

The simplest case is a type Ia SN in a uniform interstellar medium and magnetic field, with SN 1006 as the clearest example. (Fig. 1). The time-average magnetic field line geometry is schematically shown in Fig. 2 [8].

For kinematic reasons injection of suprothermal ions escaping from a thermalized downstream region can only occur for quasi-parallel shocks, where the instantaneous angle $\Theta_{nB} \ll \pi/2$. And clearly acceleration can occur only at those parts of the shock surface, where particles can be injected. Particle acceleration is also directly connected with the self-excitation of Alfvén waves which stochastically change Θ_{nB} . As a consequence we have (i) a stochastic self-limitation of the ion injection rate η through nonlinear wave

production, from $\eta_{\parallel} \approx 10^{-2}$ to an $\eta_{\text{eff}} \approx 10^{-4}$, plus (ii) a systematic reduction of η due to the overall average field morphology, i.e. strong wave production can occur only locally in the polar regions, (iii) the hadronic γ -ray emission is therefore also dipolar for uniform external field \underline{B}_1 , and (iv) the same is true for the synchrotron emission as a result of field amplification by factors between 5 and 10 in the ion acceleration regions [12, 9, 10], with essentially lower emission from the extensive equatorial region. This last consequence has been impressively proven in a recent analysis of the XMM data for SN 1006 by [11].

Altogether this injection asymmetry requires a reduction of the overall acceleration efficiency of nuclear particles as calculated in the spherically symmetric model. The reduction factor is given by the ratio of the polar areas to the total shock surface area. This ratio is about 0.2 for a case like SN 1006. In order to reach an overall acceleration efficiency of 10% this requires the shock regions in which acceleration actually occurs to achieve an acceleration efficiency of about 50%. Such a high efficiency implies an extremely nonlinear acceleration process with a strong backreaction of the accelerated particles on the shock structure.

3 Comparison with theory

The comparison with theory is of course an essential aspect. However, at present the theory is still incomplete. The full solution of the Fokker-Planck transport equations for the distribution functions $f(p, r, t)$ of nuclear particles and electrons, coupled with the hydrodynamics of the thermal plasma through the CR pressure gradient and wave dissipation, requires even in spherical symmetry the knowledge of several “unknowns”: the effective, amplified magnetic field strength B_{eff} , the actual proton injection rate η_{eff} , and the amplitude of the electron distribution. These unknowns can only be determined through an analysis of the synchrotron observations

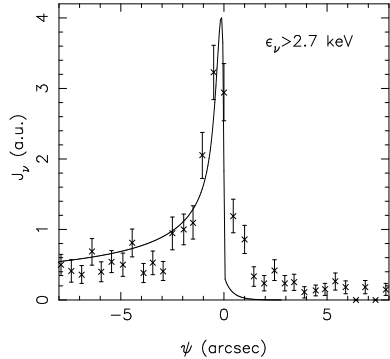


Figure 5: *Data of an individual Chandra 2-10 keV filamentary structure in Cas A and model fit to these data, interpreted as the result of strong postshock synchrotron losses (at $\psi < 0$).*

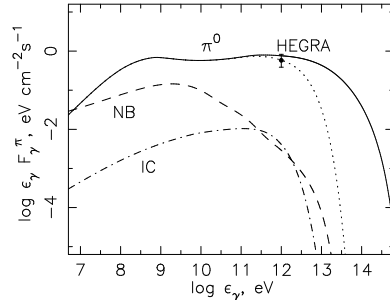


Figure 6: *Gamma-ray spectral energy density for Cas A. The (unconfirmed) HEGRA detection and the EGRET upper limit are shown together with the theoretical prediction for the π^0 -decay (full line), IC (dashed line) and NB (dash-dotted line) emissions.*

which involve the relativistic electron component. This analysis is actually possible, because for particle energies $E \gg mpc^2$, corresponding to ultra-relativistic protons, electrons behave like protons in the acceleration process (e.g. [13]).

I will only summarize the situation here.

The electrons are parasitically accelerated in an environment produced by the accelerating nuclear particles because they can not modify the shock themselves due to their small energy density. And therefore at energies $E \gg mpc^2$ their momentum distribution equals in form that of the nuclear particles except for radiative (synchrotron) losses:

- The radio synchrotron spectrum is generally steeper than in the test particle approximation, because the radiating low-energy electrons “see” only the discontinuous subshock in the thermal gas and not the full shock transition that includes

the extended CR precursor. Interpreting this effect in terms of nonlinear shock modification by the accelerated nuclear component determines the ion injection rate η_{eff}

- The energy of the radio electrons should be substantially lower than 10 mpc^2 . Together with the requirement to fit the entire synchrotron spectrum, including the cutoff at hard X-rays, this determines the (amplified) magnetic field strength B_{eff}
- The amplitude of the relativistic electron density then follows from the amplitude of the synchrotron spectrum, which fixes the electron-to-proton ratio in the accelerated CRs

4 Individual SNRs

4.1 Cas A

Cas A is presumably the result of a so-called Type Ib SN, the core collapse of a massive Wolf-Rayet star that has already shed its hydrogen envelope through a fast stellar wind (Fig. 3). In a detailed model for the thermal X-ray emission by [14] the final Wolf-Rayet wind phase has compressed the inner part of the dense slow wind from the preceding Red Supergiant (RSG) phase into a dense luminous shell; in turn the subsequent SNR shock has already reached the unperturbed RSG wind region beyond the shell.

The strong deviation of the synchrotron spectral energy density from a test particle spectrum below some tens of GHz (Fig. 4) implies a strong modification of the shock by accelerated nuclear particles, an amplified post-shock field $B_{\text{eff}} \approx 200 \mu\text{G}$, and a field $B_{\text{eff}} \approx 500 \mu\text{G}$ in the RSG wind shell [15].

The X-ray morphology of Cas A from *Chandra* also shows strongly pronounced filamentary structures of the outer shock (Fig. 5), analyzed by [16] and [17]. The multi-TeV electrons accelerated at the

shock form a very thin quasi-spherical shell – thinner than that of a children’s rubber ball – as the result of violent synchrotron cooling. This cooling scale determines the interior amplified field. It turns out that this field “measurement” agrees with that using the spectral distortion in the radio frequency range within the errors of 20 to 30 percent. Similar results have been obtained for SN 1006 [18, 19] and Tycho’s SNR [9, 10].

The theoretical prediction of the γ -ray fluxes (Fig. 6, from [15]) shows a π^0 -decay γ -ray flux that dominates those from IC scattering and NB by two orders of magnitude at 1 TeV, making it a clear hadronic γ -ray source by a large margin. This prediction essentially agrees with the flux detected by the *HEGRA* experiment [21].

The IC and NB flux determinations are quite robust results. A reliable independent measurement of the γ -ray flux with the large Northern Hemisphere telescopes *VERITAS* or *MAGIC* would therefore be of paramount importance.

4.2 SN 1006

This SNR has been observed in hard X-rays with *ASCA* to show purely nonthermal emission from the two hot spots at the poles, as discussed before, and this emission was interpreted as synchrotron radiation [2]. Later high-resolution *Chandra* and *XMM* observations strengthened this picture. However, the TeV γ -ray detections by the single *CANGAROO* telescopes *CANGAROO I* [22] and *CANGAROO II* [23] could not be confirmed in a total of 24.5 hours of observation time by the *H.E.S.S.* stereoscopic system [24]. Recent *CANGAROO* stereo observations could not detect the source any more either and have led to the withdrawal of the earlier γ -ray detection claims [25].

There are two reasons for the γ -ray non-detection. First of all, the magnetic field in the SNR interior is considerably amplified

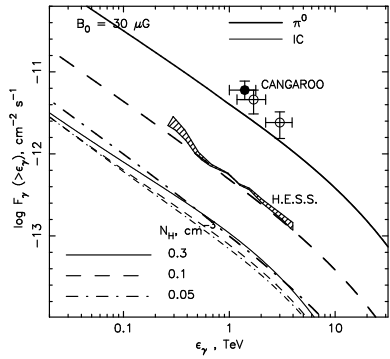


Figure 7: Integral VHE photon flux from the northeastern polar cap of SN 1006. The value $B_0 = 30 \mu G$ corresponds to an interior effective field strength of $150 \mu G$. The CANGAROO and H.E.S.S. data are shown together with the theoretical flux estimates in [19].

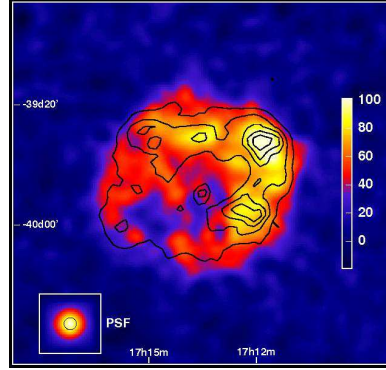


Figure 8: H.E.S.S. image of RX J1713.7-3946 at γ -ray energies ≥ 800 GeV, with the ASCA 1 – 3 keV X-ray contours superposed [20].

($B_{\text{eff}} \approx 150 \mu G$), so that the IC radiation is strongly suppressed, given the observed synchrotron emission. Secondly, the external hydrogen density N_H is in all probability quite low, $N_H < 0.1 \text{ cm}^{-3}$. Since in the Sedov phase, in which SN 1006 is at present, the π^0 -decay γ -ray flux F_γ is proportional to N_H^2 , the low gas density implies a low hadronic γ -ray emission as well. This situation has been analyzed in detail by [19]. Given the lowest value of $N_H = 0.05 \text{ cm}^{-3}$, discussed in the literature, we expect the γ -ray emission to be only a factor of 3 smaller than the present H.E.S.S. upper limit for the northeastern polar cap (Fig. 7). Since SN 1006 is the simplest case of a SNR with strong nonthermal emission in radio and X-rays and therefore the theoretically best understood object of its kind, it would obviously be important to detect it also in TeV γ -rays in a deep observation of about 200 hours with H.E.S.S. or CANGAROO.

4.3 SNR RX J1713.7-3946

Originally found in the *ROSAT* X-ray survey [26], SNR RX J1713.7-3946 was detected at VHE energies by *CANGAROO* [27] and interpreted as an IC-dominated TeV source. *ASCA* observations [28, 29] had shown that the X-ray spectrum is a purely nonthermal continuum. In 2002 the *CANGAROO* group revised its interpretation and rather favored a hadronic scenario from the shape of the TeV energy spectrum [30]. This phenomenological interpretation was questioned by [31] and [32] on the grounds that the upper limit from a nearby *EGRET* source 3EG 1714-3857, believed to be associated with the TeV source, was inconsistent with the hadronic extrapolation of the *CANGAROO* spectrum to the GeV region. Such different views were not entirely surprising at the time, considering the complex morphology of the general region in which the source is embedded. This is particularly well visible in the CO map. Nevertheless, at the present time CO data [33] give a most probable kinematic source distance of 1 kpc.

The *H.E.S.S.* experiment subsequently confirmed the *CANGAROO* detection and could give for the first time a spatially resolved VHE image of a SNR [34], whose overall shell structure correlated closely with the shell structure in *ASCA* 1–3 keV X-rays. The remnant diameter is about 1° . This was unambiguous proof for the acceleration of charged particles to energies beyond 100 TeV¹

Apart from the fit shown in Fig. 9, the *H.E.S.S.* VHE differential spectrum can be equally well fitted by a power law with exponential cutoff $\propto E^{-\Gamma} \exp^{-E/E_c}$, with $\Gamma = 1.98 \pm 0.05$ and $E_c = 12 \pm 2$. At energies $E \ll E_c$ this measured spectrum corresponds to the test particle limit of diffusive shock acceleration theory for nuclear particles in a strong shock. Even ignoring nonlinear backreaction effects the extrapolation of the charged particle spectrum to lower

¹The following discussion of this source and the figures 8 and 9 are based on the more recent *H.E.S.S.* results, not yet released at the time of the conference.

energies with a proton spectrum $\propto E^{-2}$ gives a hadronic γ -ray spectrum below an improved upper limit of *EGRET* which now assumes that RX J1713.7-3946 is not linked to the known *EGRET* source 3EG 1714-3875 [35].

Making in fact the best case for an IC interpretation by assuming a very low magnetic field strength of about $10\mu\text{G}$ inside the SNR, the resulting IC spectrum fits the *H.E.S.S.* data quite poorly. This outweighs the good correlation between the X-ray synchrotron and the γ -ray emissions which at first sight would suggest a leptonic origin of the γ -ray emission as well. In addition, already a small amplification of the magnetic field in the remnant rules out a dominant IC emission and a fortiori a dominant NB, whereas a hadronic γ -ray spectrum continues to fit the data quite well [35]. Despite the complex CO morphology and unknown age of this remnant I believe that a hadronic interpretation of the γ -ray emission from RX J1713.7-3946 is clearly favored. The most plausible acceleration scenario is that of a massive progenitor star which, over its long evolution time, had produced a large stellar wind bubble into which finally the SN exploded about a thousand years ago (see e.g. Fig. 5 of [36]). Only this makes the almost circular X-ray morphology understandable that was found by *ASCA* and *XMM* [37, 38]. And it can explain the low effective density inside the SNR [37]. A detailed theoretical model is needed to investigate the consistency of such a picture with the existing MWL evidence.

4.4 Vela Jr.

The SNR RX J0852.0-4622, also called Vela Jr., was also found with *ROSAT* [39] as a very large $2^\circ \times 2^\circ$ quasi-circular X-ray structure and later confirmed by *ASCA* [40, 41]. In the VHE range it was detected by *CANGAROO* [42] and by *H.E.S.S.* [43], see Fig. 10.

The flux above 1 TeV equals 1.4 times the flux from RX J1713.7-3946 and is about equal to the flux from the Crab Nebula. The

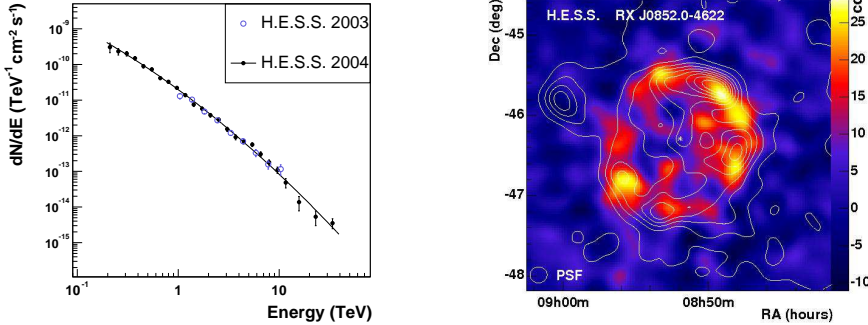


Figure 9: *H.E.S.S.* differential γ -ray spectrum of RX J1713.7-3946 for the whole region of the SNR solid black circles. The best fit of a power law with energy-dependent photon index is plotted as a black line. The *H.E.S.S.* 2003 data are given by the blue open circles. Error bars are $\pm 1\sigma$ statistical errors [35].

Figure 10: *Vela Jr.* in TeV γ -rays. The color scale is in number of γ -ray events. The total significance of this 3.2 hours lifetime observation with *H.E.S.S.* is 12σ . The source radius is four times the radius of the full Moon.

differential spectrum is a hard power law spectrum with $\Gamma = 2.1 \pm 0.1 \pm 0.1$ [43].

The physical characteristics of Vela Jr. appear to be rather similar to those of RX J1713.7-3946, even though the source may be even closer and younger. Interestingly, also a narrow filament was recently found in *Chandra* data [44]. If we interpret this filament as part of the outer SNR shock its sharpness suggests magnetic fields at least in the $100\mu\text{G}$ range, almost independently of the detailed astronomical properties of the source [45]. Therefore again a hadronic interpretation of the γ -ray emission is plausible, even though little theoretical analysis has been performed up to now. Further and more detailed results on the morphology and spectrum are expected to be available soon. They should make this source the second major VHE SNR source in the Southern Hemisphere.

5 Galactic Plane Scan SNRs, Conclusions

The *H.E.S.S.* Galactic Plane Scan [46, 47] has revealed some 20 odd new sources until now. Several of these sources can be associated with SNRs with reasonable certainty, but many of them are still unidentified at the present time. It is clear that further study of these SNRs is required, both at VHE energies and at other wavelengths. An example is HESS J1813-178 where, quickly following the initial *H.E.S.S.* publication of the first scan results, a SNR was found in existing *VLA* radio data [48], and a known coincident *ASCA* source was found also by *INTEGRAL* in the 20-100 keV band [49].

In the present context such studies are important to identify the statistical VHE properties of the Galactic SNR and thus to control whether the few very nearby objects, that can be studied in great detail, are typical representatives of this population or not.

Even though it is difficult to make such population studies in the Northern Hemisphere, there are at least two bright historical SNRs in this Hemisphere, Cas A and Tycho's SNR. Cas A has been detected by *HEGRA* in TeV γ -rays with rather low significance, whereas the *HEGRA* flux upper limit for Tycho's SNR [50] is only a factor of unity above the theoretical VHE prediction [51, 9]. Together with other known Northern Hemisphere SNRs, the confirmation/detection – or not – of these objects with *VERITAS* or *MAGIC* would be of high significance for the question of CR origin in SNRs.

Acknowledgments

I would like to thank the members of the *H.E.S.S.* collaboration for discussions about the *H.E.S.S.* and *HEGRA* results mentioned in this talk. I also gratefully acknowledge the collaboration with

E.G. Berezhko and L.T. Ksenofontov on the theory of SNRs over the years.

References

- [1] A.M. Hillas, *J. Phys. G* **31**, R95 (2005)
- [2] K. Koyama et al., *Nature* **378**, 225 (1995)
- [3] H.J. Völk, *Proc. "Towards a Major Atmospheric Cherenkov Detector-V, Kruger Nat'l Park*, ed. O.C. de Jager, Westprint-Potchefstrom, RSA, p. 87 ff (1997)
- [4] H.J. Völk, *Frontiers of Cosmic Ray Science, Proc. 28th ICRC* (Tsukuba) **8**, 29 (2003)
- [5] L.O'C. Drury et al., *Astron. Astrophys.* **287**, 959 (1994)
- [6] E. Berezhko et al., *Astroparticle Phys.* **2**, 215 (1994)
- [7] E. Berezhko et al., *J. Exp. Theor. Phys.* **82**, 1 (1996)
- [8] H.J. Völk et al., *Astron. Astrophys.* **409**, 563 (2003)
- [9] H.J. Völk et al., *Astron. Astrophys.* **433**, 2929 (2005)
- [10] J. Ballet, *Adv. Space Res.* **35**, (2005); (astro-ph/0503309)
- [11] R. Rothenflug et al., *Astron. Astrophys.* **425**, 121 (2004)
- [12] A.R. Bell, *MNRAS* **182**, 550 (2004)
- [13] E.G. Berezhko, *Adv. Space Res.* **35**, 1031 (2005)
- [14] K.J. Borkowsky et al., *Astrophys. J* **466**, 866 (1996)
- [15] E.G. Berezhko et al., *Astron. Astrophys.* **400**, 971 (2003)

- [16] J. Vink et al., *Astrophys. J.* **548**, 758 (2003)
- [17] E.G. Berezhko et al., *Astron. Astrophys.* **419**, L27 (2004)
- [18] E.G. Berezhko et al., *Astron. Astrophys.* **412**, L11 (2003)
- [19] L.T. Ksenofontov et al., *Astron. Astrophys.* **443**, 973 (2005);
(astro-ph/0508318)
- [20] D. Berge et al. (for the H.E.S.S. collaboration), *Proc. 29th ICRC* Pune (2005), **4**, 117
- [21] F.A. Aharonian et al., *Astron. Astrophys.* **370**, 112 (2001)
- [22] T. Tanimori et al., *Astrophys. J.* **497**, L25 (1998)
- [23] T. Tanimori et al., *Proc. 27th ICRC* (Hamburg) **6**, 2465 (2001)
- [24] F.A. Aharonian et al., *Astron. Astrophys.* **437**, 95 (2005)
- [25] M. Mori, *these proceedings*, p. 19 (2005)
- [26] E. Pfeffermann et al., in “*Roentgenstrahlung from the Universe*”, 267 (1996)
- [27] H. Muraishi et al., *Astron. Astrophys.* **354**, L57 (2000)
- [28] K. Koyama et al., *PASJ* **49**, L7 (1997)
- [29] P. Slane et al., *Astrophys. J.* **525**, 357 (1999)
- [30] R. Enomoto et al., *Nature* **416**, 823 (2002)
- [31] O. Reimer et al., *Astron. Astrophys.* **390**, L43 (2002)
- [32] Y.M. Butt et al., *Nature* **418**, 499 (2002)
- [33] Y. Fukui et al., *PASJ* **55**, L61 (2003)

- [34] F.A. Aharonian et al., *Nature* **432**, 75 (2004)
- [35] F.A. Aharonian et al., *Astron. Astrophys.* in press (2005); arXiv:astro-ph/0511678
- [36] E.G. Berezhko et al., *Astron. Astrophys.* **357**, 283 (2000)
- [37] G. Cassam-Chenai et al., *Astron. Astrophys.* **427**, 199 (2004)
- [38] J.S. Hiraga et al., *Astron. Astrophys.* **431**, 953 (2005)
- [39] B. Aschenbach, *Nature* **396**, 141 (1998)
- [40] H. Tsunemi et al., *PASJ* **52**, 887 (2000)
- [41] P. Slane et al., *Astrophys. J.* **548**, 814 (2001)
- [42] H. Katagiri et al., *Astrophys. J.* **619**, L163 (2005)
- [43] F.A. Aharonian et al., *Astron. Astrophys.* **437**, L7 (2005)
- [44] A. Bamba et al., *Astrophys. J.* **632**, 294 (2005)
- [45] H.J. Völk et al., *Proc. 29th ICRC* Pune (2005) **3**, 233
- [46] F.A. Aharonian et al., *Science* **307**, 1938 (2005)
- [47] F.A. Aharonian et al., *Astrophys. J.*, to appear (2005)
- [48] C.L. Brogan et al., *Astrophys. J.* **629**, L105 (2005)
- [49] P. Ubertini et al., *Astrophys. J.* **629**, L1009 (2005)
- [50] F.A. Aharonian et al., *Astron. Astrophys.* **373**, 292 (2001)
- [51] H.J. Völk et al., *Astron. Astrophys.* **396**, 649 (2002)